LARGE COLORLESS HPHT-GROWN SYNTHETIC GEM DIAMONDS FROM NEW DIAMOND TECHNOLOGY, RUSSIA

Ulrika F.S. D'Haenens-Johansson, Andrey Katrusha, Kyaw Soe Moe, Paul Johnson, and Wuyi Wang

The Russian company New Diamond Technology is producing colorless and near-colorless HPHT-grown synthetic diamonds for the gem trade. Forty-four faceted samples synthesized using modified cubic presses were analyzed using a combination of spectroscopic and gemological techniques to characterize the quality of the material and determine the means of distinguishing them from natural, treated, and alternative laboratory-grown diamonds. These samples, with weights ranging from 0.20 to 5.11 ct, had color grades from D to K and clarity grades from IF to I_2. Importantly, 89% were classified as colorless (D–F), demonstrating that HPHT growth methods can be used to routinely achieve these color grades. Infrared absorption analysis showed that all were either type IIa or weak type IIb, and photoluminescence spectroscopy revealed that they contained Ni-, Si-, or N-related defects. Their fluorescence and phosphorescence behavior was investigated using ultraviolet excitation from a long-wave/short-wave UV lamp, a DiamondView instrument, and a phosphorescence spectrometer. Key features that reveal the samples' HPHT synthetic origin are described.

In the last few years, available colorless and near-colorless gem-quality synthetic diamonds have improved dramatically with advances in growth technologies and a heightened understanding of the underlying processes. Although the majority of these products have been grown using the well-established chemical vapor deposition (CVD) technique (see Martineau et al., 2004; Wang et al., 2007; 2012), the high-pressure, high-temperature (HPHT) method, associated more with attractive fancy color samples, has recently emerged as a method for producing sizable colorless and near-colorless synthetic diamonds (D'Haenens-Johansson et al., 2014). The commercial viability of synthetic diamonds depends on a variety of factors, such as desirable colors (or, in this case, the absence of color), clarities, and sizes. Additionally, producers must be able to manufacture a high enough volume to satisfy demand at a price point that makes them competitive with natural diamond and alternative diamond products.

New Diamond Technology (NDT), which together with Inreal and Nevsky Brilliant is part of a Russian diamond group, has grown synthetic diamonds for industrial and technological uses. In the past year, the company has produced large high-quality, colorless samples for the gem trade. NDT says it has developed HPHT technology that enables the growth of multiple synthetic diamonds in different reaction layers within the same cell, resulting in much larger production runs compared to other known methods, reaching up to 200 samples (with cross-sectional sizes of 2.5–3.0 mm) across two layers in a single run. At present, NDT can simultaneously grow up to 16 colorless "rough" crystals approaching 10 ct apiece.

See end of article for About the Authors and Acknowledgments.
GEMS & GEMOLOGY, Vol. 51, No. 3, pp. 260–279,
http://dx.doi.org/10.5741/GEMS.51.3.260.

Figure 1. A: These three colorless HPHT-grown synthetic diamonds demonstrate some of the sizes achieved by New Diamond Technology. From left to right, samples NDT04, NDT02, and NDT01 weigh 2.02, 2.20, and 2.30 ct, respectively. Photo by Ulrika D'Haenens-Johansson. B: Sample NDT-A, a 5.11 ct specimen with K color, is the largest faintly colored synthetic diamond studied by GIA to date. The visual characteristics of these samples are summarized in table 1. Photo courtesy of New Diamond Technology.

It was reported in May 2015 that NDT had produced a 32.26 ct "rough" synthetic diamond, which was subsequently faceted into a 10.02 ct square-cut emerald shape and graded by the IGI Hong Kong laboratory as E color and VS_1 clarity (International Gemological Institute, 2015). This is believed to be the largest colorless synthetic diamond to date from either HPHT or CVD growth. New Diamond Technology's crystals have the potential to be faceted and polished into gems that are significantly larger than those currently available from other HPHT synthetic producers such as AOTC, which limit their polished sizes to less than 1 ct, usually about 0.5 ct (D'Haenens-Johansson et al., 2014; AOTC, 2015).

In October 2014, NDT loaned GIA a suite of 44 colorless to faintly colored polished gem-quality HPHT-grown synthetic diamonds ranging from 0.20 to 5.11 ct, representative of their 2014 production (see figure 1). The largest of these was reported in February 2015 by *JCK* magazine and by GIA researchers the following month (Bates, 2015; Poon et al., 2015). The 44 samples were comprehensively investigated using both gemological and spectroscopic techniques. Based on the results presented in this study, NDT's lab-grown samples, though often included, achieved excellent colors and could visually match high-quality natural diamonds. Nevertheless, the samples could be readily separated from natural stones by characteristics that arise from their artificial growth conditions.

BACKGROUND ON HPHT SYNTHETIC DIAMOND GROWTH

Most HPHT growth of single-crystal diamond, irrespective of the press design, is based on the temperature-gradient method first developed by Bovenkerk et al. (1959) for General Electric. The growth capsule is filled with the ingredients necessary for laboratory diamond growth: a source of carbon (such as graphite), a sacrificial diamond "seed" that acts as a template for diamond formation, and a metallic solvent/catalyst (usually Fe, Ni, Co, or their alloys). The catalyst enables diamond growth at lower temperatures and pressures than would be otherwise possible, alleviating some of the technological requirements. The capsule is then exposed to pressures of 5–6 GPa and temperatures of 1300–1600°C. The design of the system creates a temperature gradient, with the source carbon area hotter than the area where the seed is located. Consequently, the carbon is dissolved into the hot molten metal and transferred into the cooler region, where it recrystallizes in the form of synthetic diamond on the seed.

The main focus of HPHT technology development has been to create systems that can reliably produce large volumes of synthetic diamonds with desirable properties for specific technological and industrial needs. Although HPHT diamond synthesis was first achieved in the 1950s, it was only in the 1990s that certain manufacturers started growing samples for the gem and jewelry trade (e.g., Shigley

et al., 1997). Since color-producing dopants such as nitrogen (yellow) or boron (blue) are so easily introduced, these were typically fancy-color synthetics.

Creating colorless HPHT synthetics has been significantly more challenging, as costly modifications to the capsule design are necessary and additional constraints must be placed on the chemical components to minimize dopant uptake, particularly nitrogen. Eliminating contamination in the growth cell is impossible, as trace amounts of nitrogen will likely remain. Thus, growers have to adapt the growth chemistry to intentionally include elements with a strong affinity to nitrogen, termed "nitrogen getters," effectively trapping the nitrogen so it does not disperse through the diamond lattice. Finally, growth rates for high-purity colorless diamond (type IIa or weak type IIb) are significantly lower than for standard type Ib (containing isolated nitrogen) synthetic diamond, necessitating longer growth times and greater control over the temperature and pressure conditions. Consequently, successful near-colorless diamond synthesis depends on the careful design of the HPHT press and its components, the quality and chemical composition of the solvent/catalyst melt, the choice of nitrogen getters, and the ability to control the chemical and thermodynamic conditions across the reaction layer. Further complications result from the need for high crystal quality and minimal inclusion uptake.

In Brief

- The Russian company New Diamond Technology (NDT) is producing faceted colorless and near-colorless HPHT-grown synthetic diamonds for the gem trade.
- Eighty-nine percent of the 44 faceted samples, weighing up to 5.11 ct, were classified as colorless. Color and clarity grades ranged from D to K and IF to I_2.
- The quality of NDT-produced material is on par with, or surpasses, that by other synthetic diamond growers.
- The samples were conclusively identified as HPHT synthetics using a combination of gemological observations and spectroscopic analysis.

HPHT GROWTH CONSIDERATIONS BY NEW DIAMOND TECHNOLOGY

NDT uses modified cubic HPHT presses to grow gem-quality colorless synthetics, with custom-made

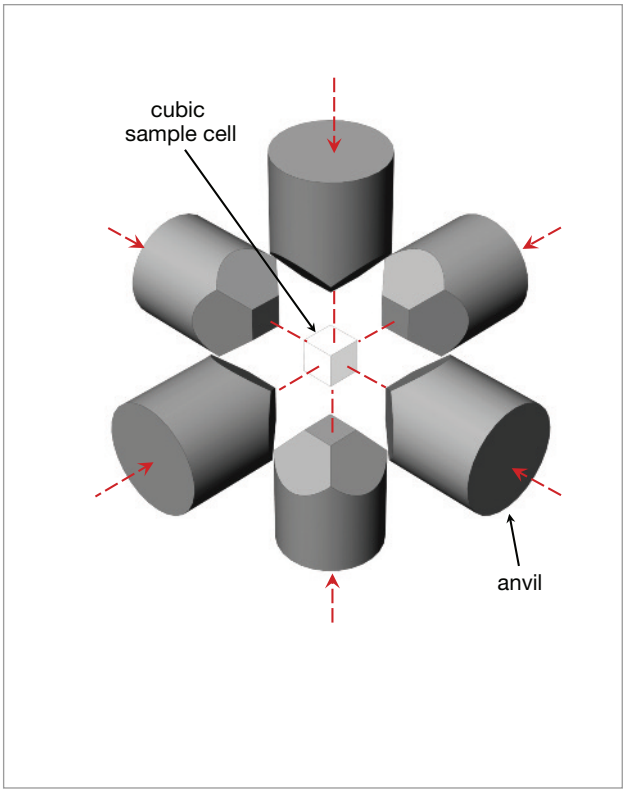

Figure 2. The anvil arrangement and sample cell for a standard cubic press. Illustration by M. Toosi and U. D'Haenens-Johansson, adapted from Sumiya (2009).

systems designed to stabilize the thermodynamic parameters (pressure and temperature distribution across the sample cell). Figure 2 illustrates the main components of a standard cubic press, which consists of six anvils coupled to independent hydraulic cylinders surrounding a cubic sample cell. Although this design is complicated by the requirement for synchronized motion of separate anvils, it does allow the application of hydrostatic pressure across a relatively large volume cell compared to other press types.

When selecting materials for the cell components of a multi-anvil apparatus, such as a cubic HPHT press, it is necessary to consider their ability to withstand the high-pressure and high-temperature conditions necessary to synthesize diamond with the desired properties. This will depend on both the compressive strength of the materials and component geometries. Generally, the choice of materials is limited to either complex ceramics (Al, Zr, or Mg oxides) or salt-based materials (iodides and chlorides) (Strong, 1977; Satoh et al., 2000; Zhu et al., 2012). Their properties, coupled with the press design, determine the producer's ability to apply long-lasting hydrostatic

Figure 3. A: In the multi-seed diamond growth layout on the left, the distribution of the temperature field was ideally controlled across the reaction layer, resulting in even growth sizes for all the samples. B: In the growth layout on the right, the temperature distribution was not optimized. The crystal edge sizes are less than 2 mm. Photos courtesy of New Diamond Technology.

pressure to the sample cell. If the designs for the cell components are not optimized, they may deteriorate during the HPHT run, hindering the stability of the growth parameters and in turn the synthesis quality. In the worst case, there may be catastrophic failure, with a component breaking. This may lead to costly damage to the equipment in addition to the cost associated with an unsuccessful growth run.

Another prerequisite for successful diamond growth is the precise control of the carbon concentration field, which is determined mostly by the temperature distribution field within the reaction volume of the cell (liquid solvent volume). Computer simulation methods such as FEM (the finite element method) are widely used to model the carbon concentration field, which defines the carbon flow direction, at different thermodynamic conditions as well as for different growth cell designs (Zhan-Chang et al., 2013). It is important to note that the correct prediction of material properties inside the reaction volume, in particular for composites, is greatly complicated by the high pressures and temperatures they are subjected to. Correct control of the temperature distribution (isotherms) inside the cell is also important, especially for layouts containing multiple seeds and/or growth layers. Examples of two separate multiple-seed growth layouts tested by NDT are shown in figure 3. These trials demonstrated that the arrangement in figure 3A resulted in a more even temperature distribution across the reaction volume, producing higher-quality crystals with more uniform size.

Care must also be taken when selecting the solvent/catalyst constituents contained within the growth cell. The chemical properties of the interaction boundary at the surface of the growing diamond crystal can determine the crystal's morphology, crystalline quality, impurity concentrations, and propensity to trap inclusions. Iron-based solvents, which include Ni and/or Co, are often used for HPHT diamond growth (Strong and Chrenko, 1971). For colorless diamond growth, it is important to suppress the introduction of boron and nitrogen impurities, which generally form color-producing substitutional defects. Traces of boron can be present in either the carbon source or the solvent/catalyst, yet careful selection of high-purity materials (with boron concentrations less than 0.1 ppm) may reduce the boron uptake to the extent that it no longer produces a discernible blue color (Sumiya and Satoh, 1996). Most diamonds will readily incorporate nitrogen present within the growth cell, which can originate from the carbon source, the solvent/catalyst, and gas found in empty spaces or pores of the capsule. This results in a high concentration of isolated nitrogen defects, which impart a yellow color. To produce a colorless diamond, nitrogen getters such as Al, Ti, Zr, or Hf are used (Sumiya and Satoh, 1996). These additives will also influence the growth properties of the material.

Using an Fe-based solvent/catalyst with the addi-

Figure 4. As-grown HPHT diamond single crystals produced using a simple Fe-based solvent with Al as a nitrogen getter. The sample on the far right is the largest, weighing 1.40 ct. Photo courtesy of New Diamond Technology.

tion of only Al results in crystal growth dominated by {100} and {111} faces, as shown in figure 4. While these are simple to facet into gems, NDT says the color grade of material produced through these methods is generally limited to G or poorer. Conversely, adding Co and Ti/Zr to the growth medium stimulates the formation of high-index growth planes such as {113}, {110}, and {115}, yet this material benefits from being colorless (D–F color grades). Unfortunately, the nitrogen getters may react with the carbon source to form carbides, which affect the carbon transport and diffusion properties of the system, decreasing the carbon available for crystal growth. These conditions may result in trapped traces of the metal/catalyst melt, forming visible inclusions. To suppress the development of such inclusions, it may be necessary to (1) introduce additional chemicals such as Cu or (2) decompose the carbides otherwise created by the nitrogen getters (Sumiya and Satoh, 1996; Sumiya et al., 2002). Obtaining sufficiently pure constituent metals for the solvent/catalyst may be challenging, necessitating additional purification steps by the manufacturer. The identities and incorporation methods for the nitrogen getters and other additives vary for different manufacturers and research teams, and the ultimate mix of solvent/catalyst and getter is often proprietary. NDT claims to have determined the optimal balance of chemical constituents needed to routinely produce gem-quality colorless synthetic diamonds, divulging that their solvent is based on Fe, Co, or a combination of the two.

Orientation of the seed initiation surface also significantly affects the morphology of the grown crystals (figure 5). Using differently oriented seeds—with {110}- or {113}-oriented initiation surfaces, for example—may optimize the growth morphology. To grow a crystal whose top face is {110}- or {113}-oriented, it is not strictly necessary to have a seed with a similarly oriented face, only to have the [110] or [113] di-

Figure 5. The morphology of synthetic diamonds depends largely on the orientation of the seed surface. Photo A shows a reaction layer where the sample in the center and the two outer rings of samples were grown on {100}-oriented seeds. Meanwhile, the samples with triangular outlines (the two inner rings) were grown using {111}-oriented surfaces. The samples shown here are yellow due to the presence of isolated nitrogen. The blue samples shown in (B) and (C) are boron-doped and were grown on {100}- and {111}-oriented substrates, respectively. The samples shown in (B) weigh 0.92 and 0.23 ct, while those in (C) weigh 0.29 and 0.88 ct. Photos courtesy of New Diamond Technology.

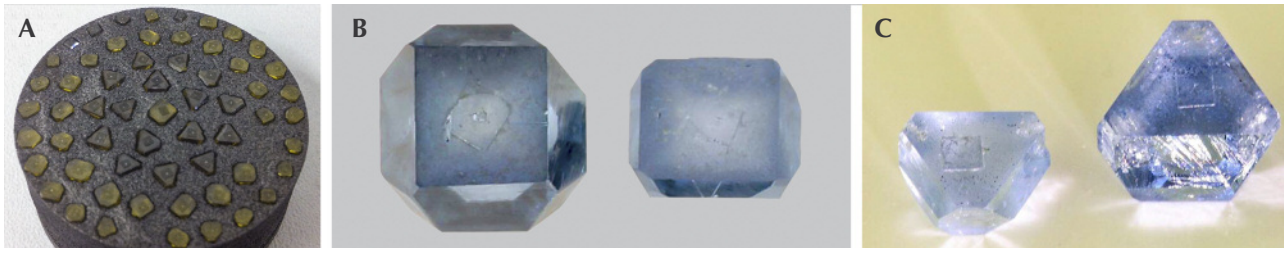

rection vertical in the growth chamber. Since seed crystals are typically cuboctahedral, however, it is easier to orient them in the chamber with either a (100) or (111) face on the top. Consequently, most HPHT diamond growth is conducted on (100)- or (111)-oriented seeds. NDT generally uses the former, which produce crystals with higher cutting yields and more easily polished surfaces.

The growth rate of individual diamond crystals depends on a combination of parameters: the identities and ratios of the chemical constituents used for growth; the thermodynamic conditions; the seed quantity, size, and orientation; the carbon flow rate; and temperature gradient. The quantity of the seeds in a run can greatly impact the growth rate of individual crystals if no additional changes are made to the cell, with an increase in the number of crystals leading to a slower rate. The latter parameter is adjusted by modifying the growth cell layout. When evaluating growth rates quoted by manufacturers, it is important to note that the rate increases nonlinearly with crystal mass. As the crystal grows, the surface area (and hence the deposition area) increases. Yet the deposition rate per unit area (mm/hour) is approximately constant. Consequently, the crystal growth rate (mg/hour) for a given area will rise (Sumiya et al., 2005). Colorless type IIa diamond growth rates as high as 8–10 mg/hour can be achieved using HPHT technology, though such material is generally plagued by metallic inclusions (Sumiya et al., 2005). Limiting the maximum stable growth rate to 6–7 mg/hour has been reported to produce higher-quality growth (Sumiya et al., 2005).

NDT systems can support growth for 200–250 hours, simultaneously yielding up to 16 crystals weighing up to 10 ct each. Further modifications have enabled growth rates up to 30–50 mg/hour—up to five times higher than commonly reported—though maintaining this rate for extended periods is challenging due to the higher pressure and temperature conditions required.

MATERIALS AND METHODS

For this investigation, NDT loaned GIA 44 colorless to faintly colored HPHT-grown specimens. These samples had been faceted into round brilliant (26) or fancy shapes (18) and weighed 0.20–5.11 ct (table 1; see again figure 1). According to NDT, these samples were grown separately using cubic presses in single-layer runs, and are representative of their 2014 production methods. Because of limited access times, the two largest samples, labeled NDT-A (5.11 ct) and NDT-B (4.30 ct), underwent fewer tests than the rest of the samples, as specified below.

Color and clarity grading was performed by GIA using standard diamond grading nomenclature. Samples and their internal features were further examined using a standard Gem Instruments binocular microscope system and a Nikon SMZ1500 research microscope under darkfield and fiber-optic illumination. The presence of anomalous birefringence patterns, attributed to strain in the diamond lattice, was evaluated by viewing each sample between crossed polarizing filters using brightfield illumination.

The specimens' fluorescence and phosphorescence response to ultraviolet (UV) light from a conventional four-watt combination long-wave (365 nm) and short-wave (254 nm) lamp was tested in a dark room. The emission intensities were visually compared to the fluorescence of a GIA fluorescence master set. Fluorescence and phosphorescence imaging was conducted using a DTC DiamondView instrument (illumination wavelengths <230 nm), revealing the samples' internal growth structures. An in-house custom-built phosphorescence spectrometer consisting of an Ocean Optics HR4000 spectrometer coupled by fiber optics to an Avantes-DH-S deuterium-halogen light source (operating with only the deuterium light, 215–400 nm) was used to further investigate the samples' phosphorescence at room temperature (see Eaton-Magaña et al., 2007, 2008). Consecutive spectra, each with a one-second integration time, were collected for up to five minutes following 30 seconds of illumination. Samples NDT-A and NDT-B were investigated with the UV lamp and the DiamondView, but phosphorescence spectra were not recorded for them.

To gain an understanding of the impurities present in the samples, Fourier-transform infrared (FTIR) absorption spectra covering the 400–6000 cm^{-1} range were taken using a Thermo Nicolet Nexus 6700 spectrometer furnished with KBr and quartz beam splitters and a diffuse-reflectance infrared Fourier transform (DRIFT) accessory. The instrument and sample chambers were purged with dried air to minimize absorption features stemming from atmospheric water. Spectra were normalized based on the height of the two-phonon absorption in diamond (Palik, 1985), enabling us to calculate the absorption coefficient for comparison and quantitative impurity concentration analysis without having to know the light path length through the samples.

Supplementary analysis of impurity content was provided by photoluminescence (PL) spectra acquired

TABLE 1. Gemological properties and calculated bulk concentrations of neutral boron (B^0) impurities for 44 HPHT synthetic diamonds produced by New Diamond Technology.

Sample	Carat weight (ct)	Color	Clarity	Cut	Dimensions (mm)	Type	B^0 bulk concentration (ppb)
NDT-A	5.11	K	I_1	Cut-corner rectangular modified brilliant	10.05 × 8.74 × 7.01	IIb	1.2 ± 0.2
NDT-B	4.30	D	SI_1	Cushion	10.29 × 9.76 × 5.39	IIb	7 ± 1
NDT01	2.30	E	SI_1	Cushion	7.30 × 8.48 × 4.85	IIa	nd [a]
NDT02	2.20	E	VVS_2	Heart	8.53 × 7.55 × 5.41	IIb	20 ± 3
NDT03	2.03	F	SI_2	Heart	7.73 × 8.41 × 5.07	IIb	5 ± 1
NDT04	2.02	D	I_1	Pear	7.14 × 10.80 × 4.45	IIb	6 ± 1
NDT05	1.90	F	VS_1	Octagonal	7.65 × 7.68 × 4.58	IIa	nd
NDT06	1.53	D	SI_1	Round	7.18 × 7.26 × 4.60	IIb	2.0 ± 0.5
NDT07	1.53	D	I_1	Round	6.49 × 9.33 × 4.08	IIb	13 ± 2
NDT08	1.50	E	SI_1	Round	7.14 × 7.17 × 4.44	IIb	2.6 ± 0.5
NDT09	1.41	D	VS_2	Square emerald	6.25 × 6.49 × 4.26	IIa	nd
NDT10	1.20	E	SI_2	Round	6.73 × 6.75 × 4.23	IIb	2.5 ± 0.5
NDT11	1.13	D	IF	Round	6.57 × 6.62 × 4.10	IIb	0.8 ± 0.2
NDT12	1.04	E	SI_2	Oval	5.58 × 7.92 × 3.40	IIb	13 ± 2
NDT13	1.03	D	SI_2	Round	6.39 × 6.47 × 3.99	IIb	9 ± 1
NDT14	1.02	F	SI_1	Round	6.45 × 6.49 × 4.06	IIb	58 ± 9
NDT15	1.01	D	VS_2	Oval	5.64 × 7.79 × 3.35	IIb	0.5 ± 0.3
NDT16	1.00	G	I2	Round	6.50 × 6.53 × 3.79	IIb	6 ± 1
NDT17	0.92	E	VS_2	Round	6.04 × 6.07 × 3.96	IIb	1.6 ± 0.5
NDT18	0.90	D	VS_1	Pear	5.38 × 7.78 × 3.38	IIa	nd
NDT19	0.90	D	SI_1	Round	6.15 × 6.18 × 3.78	IIb	5 ± 1
NDT20	0.81	D	VVS_2	Round	5.92 × 5.96 × 3.79	IIb	2.5 ± 0.5
NDT21	0.80	D	VVS_2	Round	6.07 × 6.09 × 3.57	IIa	nd
NDT22	0.80	D	SI_2	Pear	5.34 × 7.78 × 3.17	IIb	9 ± 1
NDT23	0.71	D	VS_1	Round	5.75 × 5.80 × 3.42	IIb	8 ± 1
NDT24	0.71	D	VVS_1	Pear	5.08 × 7.29 × 2.99	IIb	6 ± 1
NDT25	0.64	E	SI_2	Round	5.43 × 5.46 × 3.53	IIa	nd
NDT26	0.58	H	I_1	Round	5.43 × 5.46 × 3.53	IIb	2.5 ± 0.5
NDT27	0.58	E	SI_2	Oval	4.89 × 6.49 × 2.75	IIa	nd
NDT28	0.54	E	SI_1	Pear	4.62 × 6.63 × 2.92	IIb	13 ± 2
NDT29	0.52	E	VS_2	Round	5.09 × 5.11 × 3.31	IIb	9 ± 1
NDT30	0.51	D	VVS_1	Round	5.15 × 5.17 × 3.90	IIb	6 ± 1
NDT31	0.50	E	SI_2	Round	5.08 × 5.12 × 3.10	IIa	nd
NDT32	0.48	D	VVS_2	Round	5.11 × 5.14 × 3.06	IIa	nd
NDT33	0.47	H	IF	Emerald	3.93 × 4.71 × 2.67	IIb	33 ± 5
NDT34	0.43	F	I_1	Round	4.78 × 4.80 × 2.99	IIb	3.7 ± 0.5
NDT35	0.43	D	VS_1	Pear	4.38 × 6.22 × 2.66	IIb	20 ± 3
NDT36	0.38	F	I_1	Round	4.70 × 4.73 × 2.83	IIb	1.8 ± 0.5
NDT37	0.37	D	I_1	Marquise	3.90 × 7.64 × 2.24	IIb	25 ± 4
NDT38	0.31	E	VS_2	Round	4.35 × 4.37 × 2.63	IIb	18 ± 3
NDT39	0.30	E	I_2	Round	4.34 × 4.36 × 2.59	IIb	1.6 ± 0.5
NDT40	0.28	F	VVS_2	Round	4.15 × 4.17 × 2.60	IIb	13 ± 2
NDT41	0.24	D	SI_1	Round	4.09 × 4.11 × 2.41	IIb	3.3 ± 0.5
NDT42	0.20	G	VS_1	Round	3.70 × 3.69 × 2.33	IIb	33 ± 5

[a] *"nd" indicates that boron was not detected.*

with the samples submerged in liquid nitrogen (77 K, or –196°C) using a Renishaw InVia Raman confocal microspectrometer (Hall et al., 2010). To maximize the effectiveness of stimulating different luminescent defect centers across a wide range of wavelengths, the system was equipped with four laser sources producing six different excitation wavelengths: He-Cd metal vapor (324.8 nm), Ar-ion (457.0, 488.0 and 514.5 nm), He-Ne (632.8 nm), and a diode laser (830.0 nm). Spectra with the 324.8 and 488.0 nm excitations were not collected for samples NDT-A and NDT-B, because of limited access to the instrument.

RESULTS AND ANALYSIS

Visual Appearance. The grading characteristics of NDT's faceted HPHT-grown diamonds are presented in table 1. The samples had carat weights ranging from 0.20 to 5.11 ct, with average and median weights of 1.08 ct and 0.81 ct. There was no clear trend between the cut shapes and sample weights, though it was noted that the six stones weighing over 2 ct were all faceted into fancy shapes. Thirty-nine (89%) of the samples were found to be colorless (D–F), while four attained near-colorless (G or H) grades and the remaining (and largest) sample was a faintly colored K grade. Remarkably, five of the six 2+ ct stones were colorless, and the color zoning often seen in HPHT-grown diamonds was not apparent. There was a wide clarity range for this set of samples: internally flawless (2, or 5%); very, very slightly included (7, or 16%); very slightly included (10, or 23%); slightly included (16, or 36%); and included (9, or 20%). No correlation was observed between sample weight, color, and clarity grade. NDT11 weighed 1.13 ct and achieved D color and IF clarity grades, marking a major breakthrough in laboratory growth.

Poorer clarity grades generally stemmed from the presence of inclusions, which appeared dark and opaque in transmitted light and gray and metallic in reflected light. These inclusions took a variety of shapes (as demonstrated in figure 6), sometimes within the same sample. Rod-like inclusions were noted to have lengths of up to approximately 1.5 mm, and could be observed singly or in clusters with the inclusions aligned in one direction. Three of the synthetics contained flat plate inclusions with approximately triangular geometry, with thicknesses of about 30 µm and edge dimensions up to approximately 600 µm. Some of the metallic inclusions were irregular in shape. Sufficiently included samples (VS_2–I_2) were attracted to a strong magnet, depending on the magnet's placement relative to the position of the inclusion. The presence of feathers, occasionally combined with metallic inclusions, also reduced the clarity grades of some samples. The inclusions likely result from entrapped traces of the metallic

Figure 6. Inclusions observed in some of New Diamond Technology's HPHT synthetic diamonds had a dark metallic appearance, suggesting they were remnants of the metallic solvent/catalyst melt used for growth. The inclusions took a variety of morphologies, including rods (A–D), thin plates (E), and irregular shapes (F). Images A, B, C, D, E, and F were taken for samples NDT16, NDT25, NDT13, NDT12, NDT26, and NDT37, respectively. Photomicrographs by Ulrika D'Haenens-Johansson.

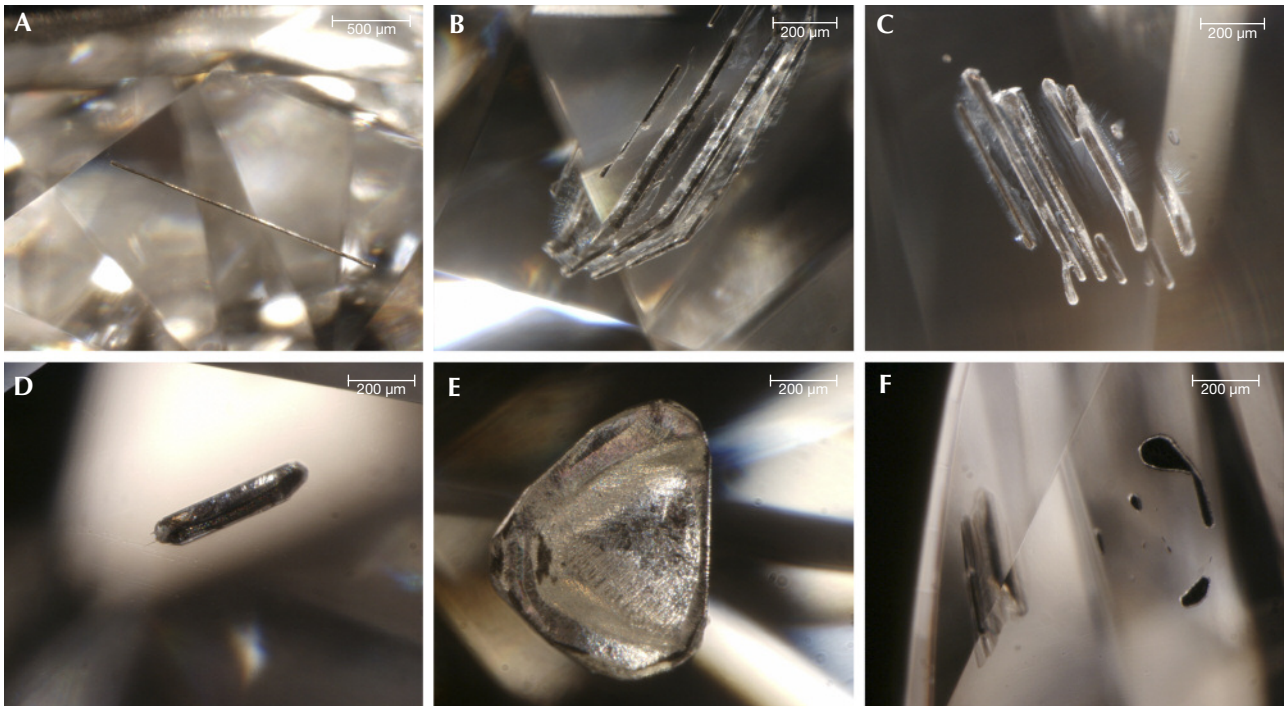

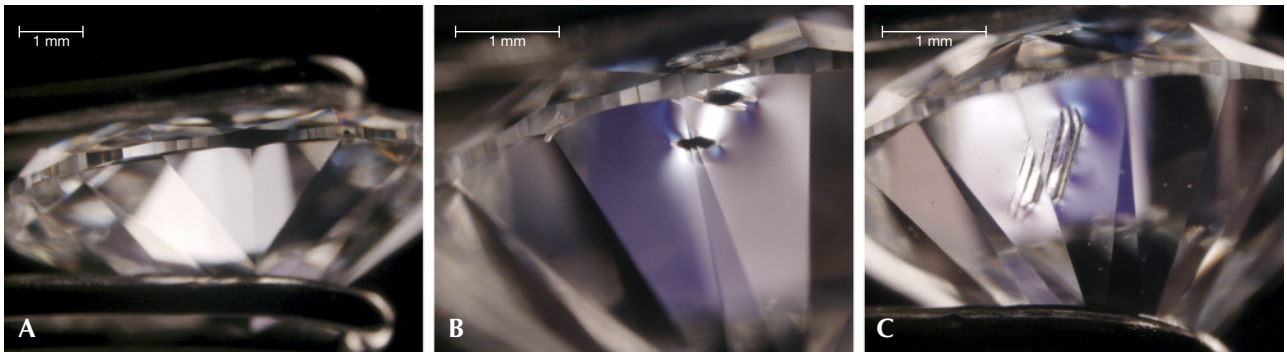

Figure 7. A: Unincluded sections of the HPHT synthetic samples did not show birefringence patterns when viewed under crossed-polarized light, instead showing smooth gradations in subdued low-order interference colors (grays, purples, and blues), indicating low levels of strain. B and C: Localized distortions in the diamond lattice were only apparent adjacent to inclusions or feathers. These images were taken for samples NDT27, NDT13, and NDT25, respectively. Photomicrographs by Ulrika D'Haenens-Johansson.

solvent/catalyst melt. Graining, an optical phenomenon whereby a series of transparent, tightly spaced lines can be observed in the sample when viewed from certain directions, has been reported in fancy-color HPHT-grown synthetic diamonds (Shigley et al., 2004) but was not detected in any of the samples in this study.

Birefringence. When viewed between crossed polarizers, the samples only showed subdued low-interference colors (grays, blues, and purples) without forming any patterns. This was in stark contrast with natural diamonds in general, which show mottled, banded, or cross-hatched "tatami" patterns in a wider range of colors. These colors, and the absence of a clear pattern, indicate that the synthetic material was characterized by low strain levels, in agreement with previously reported observations (Crowningshield, 1971; Shigley et al., 1997; D'Haenens-Johansson et al., 2014). Localized areas of higher strain were only observed adjacent to inclusions or feathers, where the diamond lattice was distorted to accommodate the clarity feature. Characteristic birefringence effects are shown in figure 7.

Fluorescence and Phosphorescence Behavior. The samples' fluorescence and phosphorescence responses to long-wave (365 nm) and short-wave (254 nm) UV illumination from a gem-testing lamp were investigated, with the results summarized in table 2. The majority (38, or 86%) were inert to long-wave UV light, with the remaining samples only emitting very faint yellow-orange fluorescence. The sample set had a stronger response to short-wave (254 nm) UV illumination, with 41 of them (93%) fluorescing yellow, orangy yellow, or green-yellow, with intensities that were very weak (22), weak (15), medium (2), or strong (1). The remaining three samples (7%) did not fluoresce. After short-wave UV illumination, 43 (98%) of the samples, including two that did not show fluorescence, displayed varying degrees of persistent green, yellowish green, greenish yellow, yellow, or orangy yellow phosphorescence, which could be observed for up to approximately six minutes. Only one sample, NDT30, showed neither fluorescence nor phosphorescence when exposed to either UV emission wavelength from the gem testing lamp. The stronger fluorescence following short-wave UV illumination is characteristic of colorless and near-colorless HPHT synthetic diamonds, the opposite of the behavior seen for natural stones (Crowningshield, 1971; Rooney et al., 1993; Shigley et al., 1997; D'Haenens-Johansson et al., 2014).

The above band-gap energy UV source (<230 nm) from a DiamondView was able to induce blue fluorescence and phosphorescence in all the samples, as illustrated in figure 8. It was crucial to view the samples along several different directions in order to perceive the cuboctahedral growth patterns characteristic of HPHT synthetic diamonds (Welbourn et al., 1996; D'Haenens-Johansson et al., 2014). The patterns were usually most clear when viewed along the pavilion, rather than with the sample oriented face-up. The patterns, which arose from the different impurity uptake efficiencies for the separate growth sectors, showed poor contrast due to the high purity levels of the samples.

TABLE 2. Fluorescence and phosphorescence behavior of the HPHT synthetics under different excitation sources.

	Long-wave (365 nm) UV gem lamp illumination response		Short-wave (254 nm) UV gem lamp illumination response		Phosphorescent emission following broadband illumination	
Sample	Fluorescence	Phosphorescence	Fluorescence	Phosphorescence	500 nm	575 nm
NDT-A	None	None	Strong yellow-green	Medium green-yellow	N/A*	N/A
NDT-B	None	None	Strong yellow-green	Strong green-yellow	N/A	N/A
NDT01	None	None	Weak green	Weak yellow	✓	×
NDT02	None	None	Weak green	Weak yellow	✓	×
NDT03	Very weak yellow-orange	Very weak yellowish orange	Weak green	Weak yellow	✓	✓
NDT04	None	None	Weak green	Very weak yellow	✓	×
NDT05	None	None	Weak green	Weak yellow	✓	×
NDT06	Very weak yellow-orange	Very weak yellowish orange	Weak yellowish green	Weak yellow	✓	✓
NDT07	None	Weak yellowish orange	Weak green	Weak yellow	✓	×
NDT08	Very weak yellow-orange	Weak yellowish orange	Weak yellowish green	Weak yellow	✓	✓
NDT09	None	None	Weak green	Very weak yellow	✓	×
NDT10	Very weak yellow-orange	Weak green	Weak green	Weak yellow	✓	✓
NDT11	None	None	Weak green	Very weak yellow	✓	×
NDT12	None	Weak yellowish orange	Weak green	Weak yellow	✓	✓
NDT13	None	None	Weak green	Very weak yellow	✓	×
NDT14	None	Very weak yellowish orange	Weak green	Very weak yellow	✓	✓
NDT15	None	None	Very weak yellowish green	Very weak yellow	✓	×
NDT16	Very weak yellow-orange	Very weak yellowish orange	Weak yellowish green	Weak yellow	✓	✓
NDT17	None	Weak yellowish orange	Weak green	Weak yellow	✓	✓
NDT18	None	None	Weak green	Very weak yellow	✓	×
NDT19	Very weak yellow-orange	None	Weak green	Very weak yellow	✓	×
NDT20	None	Very weak yellowish orange	Very weak green	Very weak yellow	✓	✓
NDT21	None	None	Weak green	Very weak yellow	✓	×
NDT22	None	None	Weak green	Very weak yellow	✓	×
NDT23	None	None	Very weak green	Very weak yellow	✓	×
NDT24	None	Very weak yellowish orange	Weak green	Very weak yellow	✓	×
NDT25	None	None	Very weak green	Very weak yellow	✓	×
NDT26	None	None	Weak yellowish green	Weak yellow	✓	×
NDT27	None	None	Weak green	Weak yellow	✓	×
NDT28	None	Very weak yellowish orange	Weak green	Weak yellow	✓	✓
NDT29	None	None	Very weak greenish yellow	Very weak orangy yellow	✓	✓
NDT30	None	None	Very weak yellow	None	✓	×
NDT31	None	None	Weak orangy yellow	Very weak Yellow	✓	×
NDT32	None	None	Weak green	Very weak yellow	✓	×
NDT33	None	None	Medium green	Medium yellow	✓	×
NDT34	None	None	None	None	✓	✓
NDT35	None	None	Very weak green	Very weak yellow	✓	×
NDT36	None	None	Very weak yellowish green	Very weak yellow	✓	×
NDT37	None	Very weak yellowish orange	Very weak green	Very weak yellow	✓	×
NDT38	None	None	Very weak yellowish green	Very weak yellow	✓	×
NDT39	None	None	Very weak orangy yellow	Very weak yellow	✓	×
NDT40	None	None	Weak yellow	Weak yellow	✓	✓
NDT41	None	None	Very weak greenish yellow	None	✓	×
NDT42	None	None	Medium yellowish green	Medium yellow	✓	×

**N/A: Not analyzed.*

The phosphorescence behavior of samples NDT01–NDT42 (totaling 42) was further investigated by collecting phosphorescence spectra at room temperature following broadband illumination (215–400 nm), collecting spectra every second with 1 second integration times. All the samples emitted blue light centered at approximately 500 nm (2.5 eV), with 13 (31%) of the specimens also showing a yellow phosphorescence band centered at about 575 nm (2.1 eV), as listed in table 2. Figures 9A and B demonstrate representative spectra for samples showing phosphorescence only from the 500 nm band (NDT37) or

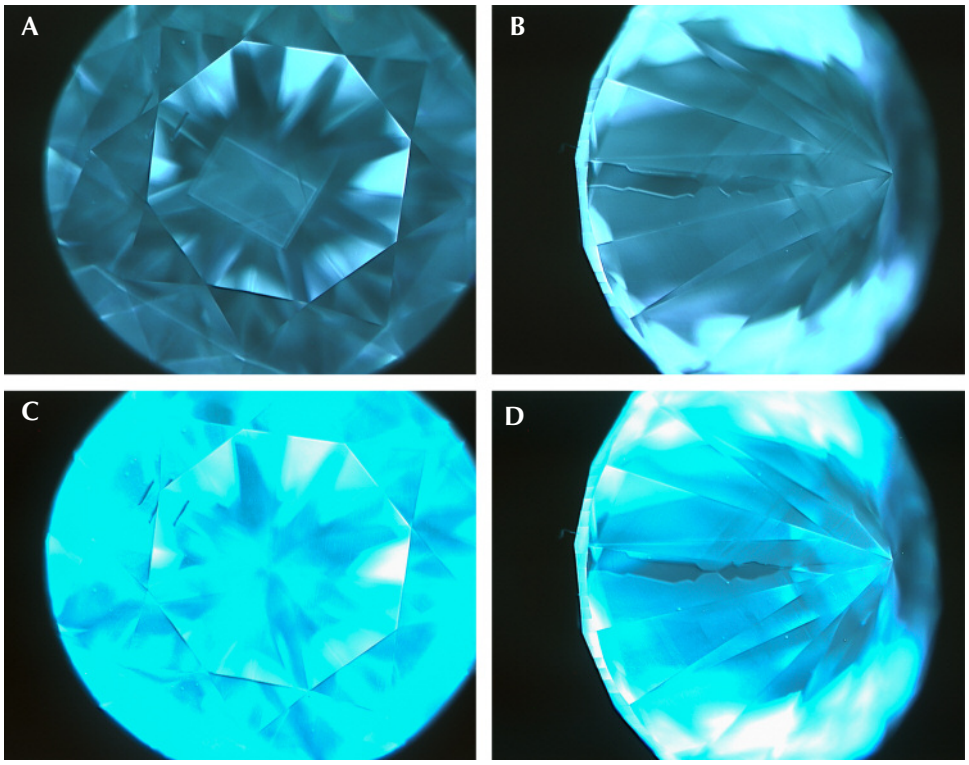

Figure 8. Blue fluorescence (A–B) and phosphorescence (C–D) were detected for all the New Diamond Technology synthetics observed with the DiamondView. Most of the samples showed cuboctahedral growth patterns characteristic for HPHT synthetics, though they were not always easily observed. The fluorescence and phosphorescence (following a 0.10 second delay) images found here were taken for sample NDT06 with 0.12 and 1.00 second exposures, respectively. Images by Ulrika D'Haenens-Johansson.

from both the 500 nm and 575 nm bands (NDT08). Phosphorescent emission at 500 nm is commonly observed in natural type IIb or weakly boron-containing type IIa diamonds, as well as similarly typed HPHT synthetic diamonds grown using a variety of solvent/catalyst melts (Watanabe et al., 1997; Eaton-Magaña et al., 2008; Eaton-Magaña and Lu, 2011; D'Haenens-Johansson et al., 2014), whereas the 575 nm band has been detected for HPHT synthetic type IIb diamonds grown using Co- and Ti-containing solvent/catalysts (Watanabe et al., 1997; Eaton-Magaña et al., 2008). A band at 580 nm has been observed in some natural type IIb diamonds, yet this band is generally very weak and rapidly decaying, making its observation rare. Neither of these bands have been reported for phosphorescent CVD synthetics (Wang et al., 2012). The 500 and 575 nm bands are induced following illumination with wavelengths less than approximately 400 nm (>3.1 eV) and 540 nm (>2.3 eV), respectively, and are thought to originate from donor-acceptor pair recombination between boron acceptors and donors, where the identity of the donor(s) is still being questioned (Watanabe et al., 1997). The main candidate for the 500 nm band is a nitrogen-related center, possibly isolated nitrogen, as it is likely present in all the types of natural and synthetic diamonds for which this phosphorescence is observed (Dean, 1965, 1973; Klein et al., 1995; Watanabe et al., 1997). The donor for the 575 nm band is much less certain (Watanabe et al., 1997). If one assumes the same donor for both bands, the energy separation between the 500 nm and 575 nm bands cannot be simply explained by a distance distribution between the donors and acceptors. Instead, it is possible that the two bands involve distinct deep donors. The donor for the 575 nm band may be a different nitrogen-related center, or even a center consisting of an impurity atom with or without nitrogen. Watanabe et al. (1997) noted that the 575 nm band was mainly emitted from regions close to the seed crystal, where faster growth rates were suspected, suggesting a higher probability of incorporating impurities from the solvent/catalyst.

Comparison of the decay of the 500 nm and 575 nm bands for the NDT samples (e.g., figure 9) revealed that the latter band is longer-lived, in agreement with published results (Watanabe et al., 1997). Consequently, the samples' phosphorescence was noted to shift from blue to yellow following illumination with the spectrometer's light source. Revisiting the samples' phosphorescence behavior under the UV gem lamp (table 2), those that displayed the most intense 575 nm bands (relative to the 500 nm band) often exhibited yellowish orange phosphorescence following long-wave (365 nm) excitation. Both the long- and short-wave UV lamps generated suffi-

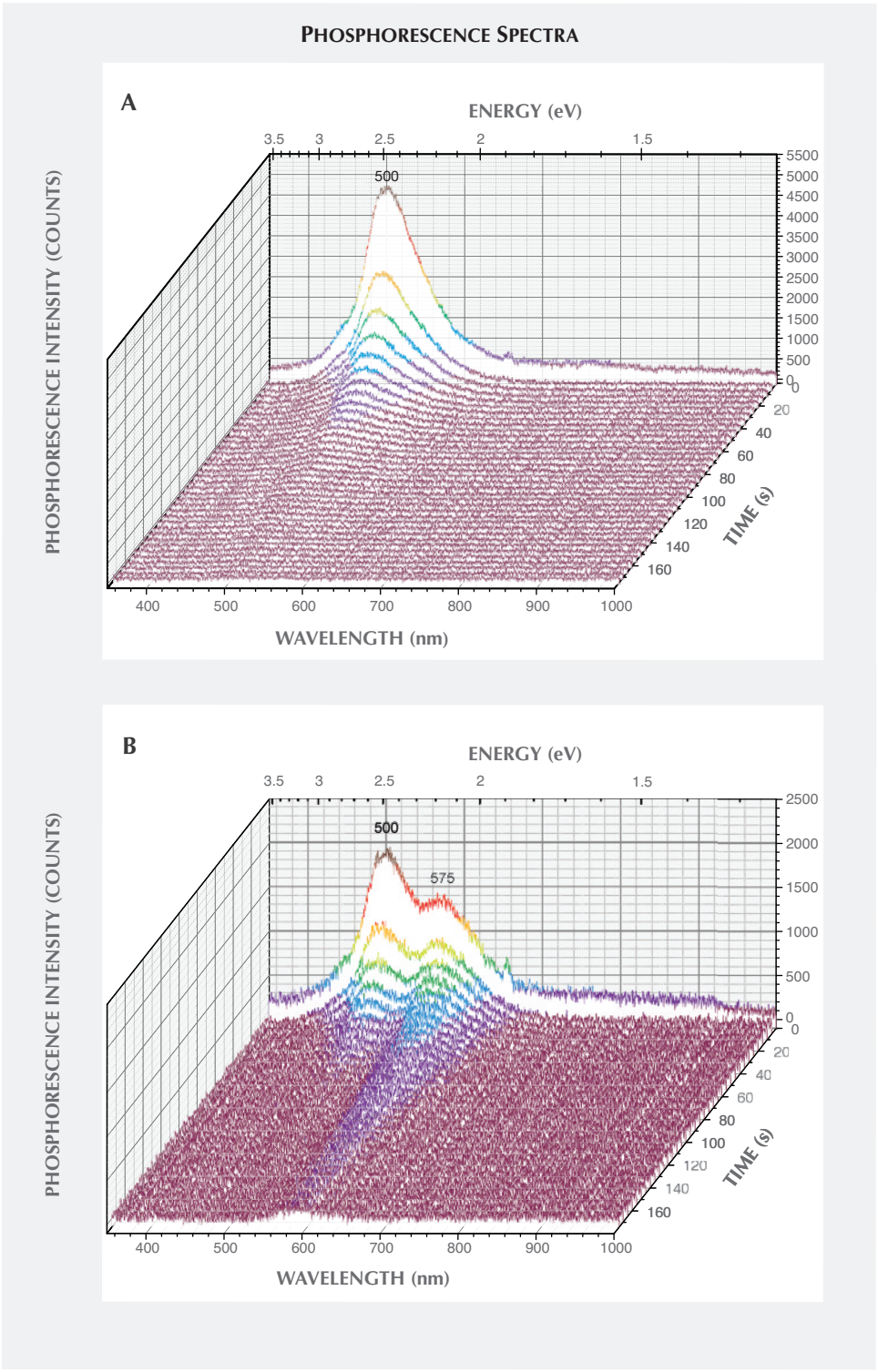

Figure 9. Room-temperature phosphorescence spectra were collected at room temperature for HPHT synthetic samples NDT01–NDT42. All 42 showed phosphorescence following illumination with broadband UV light (215–400 nm); here the spectra for the representative samples NDT37 (A) and NDT08 (B) are shown. For clarity, data is only presented for five-second intervals, even though data was collected every second. A phosphorescent emission band was detected at 500 nm for all specimens (A and B), with an additional band centered about 575 nm being observed for 13 (31%) of the samples (B). For the cases where both bands were detected, it was noted that directly following illumination, the 500 nm band dominated, with the 575 nm band displayed as a shoulder. The 575 nm band had a slower decay, and its emission could be observed even after the 500 nm emission had decayed beyond detection.

ciently high energy to induce phosphorescence from both bands (Watanabe et al., 1997).

The phosphorescence duration is affected by both the maximum phosphorescence intensity, which can be influenced by the size of the stone, and the rate of decay for the emission band(s). Since phosphorescence spectra were collected, it was possible to determine the half-life (τ) of the phosphorescence, or

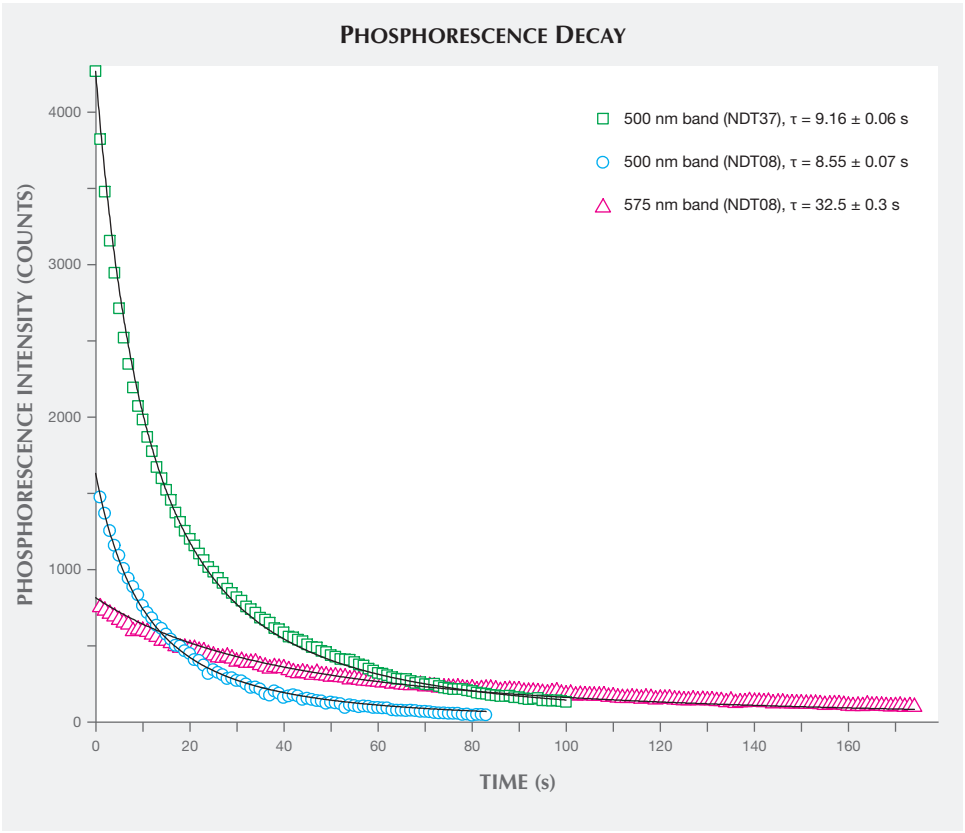

Figure 10. Phosphorescence intensity as a function of time for the 500 and 575 nm bands for samples NDT37 and NDT08. The circle, square, and triangle data points were determined from the experimental data presented in figure 9. The lines illustrate the fits obtained to these data using least-squares fitting based on the hyperbolic function expressed by equation 2, from which the half-life values τ were calculated using equation 3.

the time it took for the bands' intensities to halve. Importantly, the half-life is a measure that is independent of the initial phosphorescence intensity. The shape of the decay curve (the maximum band intensity as a function of time) can also provide information regarding the mechanism responsible for the phosphorescence. Figure 10 presents the phosphorescence decay data for the 500 and 575 nm bands for samples NDT08 and NDT37, selected for their intense phosphorescence. The bands' maximum intensities were estimated by fitting Voigt functions to the intensity data plotted as a function of energy, where energy E (in eV) and the wavelength λ (in meters) are related by

$$E = \frac{hc}{\lambda} \qquad (1)$$

where h is Planck's constant ($4.13566733 \times 10^{-15}$ eVs) and c is the speed of light (2.99792458×10^{8} m/s). The phosphorescence intensity as a function of time $I(t)$ was best modeled using a hyperbolic function

$$I(t) = \frac{I(0)}{(1+kt)^2} \qquad (2)$$

where t is the time following the extinction of the illumination, $I(0)$ is phosphorescence intensity at t = 0, and k parameterizes the phosphorescence recombination (Watanabe et al., 1997). The observation that a hyperbolic "bimolecular" curve fit better than an exponential decay is consistent with the donor-acceptor pair recombination mechanism that has been used to explain the phosphorescence of diamond (Watanabe et al., 1997). The least-squares fits to the data, as illustrated in figure 10, provided estimates for k. Setting $I(t)/I(0) = ½$ and rearranging equation 2, the half-life is then defined by

$$\tau = \frac{\sqrt{2}-1}{k} \qquad (3)$$

Thus the half-life for the 500 nm phosphorescence band for sample NDT37 (one-band emission) was calculated to be 9.16 ± 0.06 s. In sample NDT08 (two-band emission), the half-life was 8.55 ± 0.07 s for the 500 nm band and 32.5 ± 0.3 s for the 575 nm band.

FTIR Absorption Spectroscopy. FTIR spectroscopy was used to evaluate the samples' boron- and nitro-

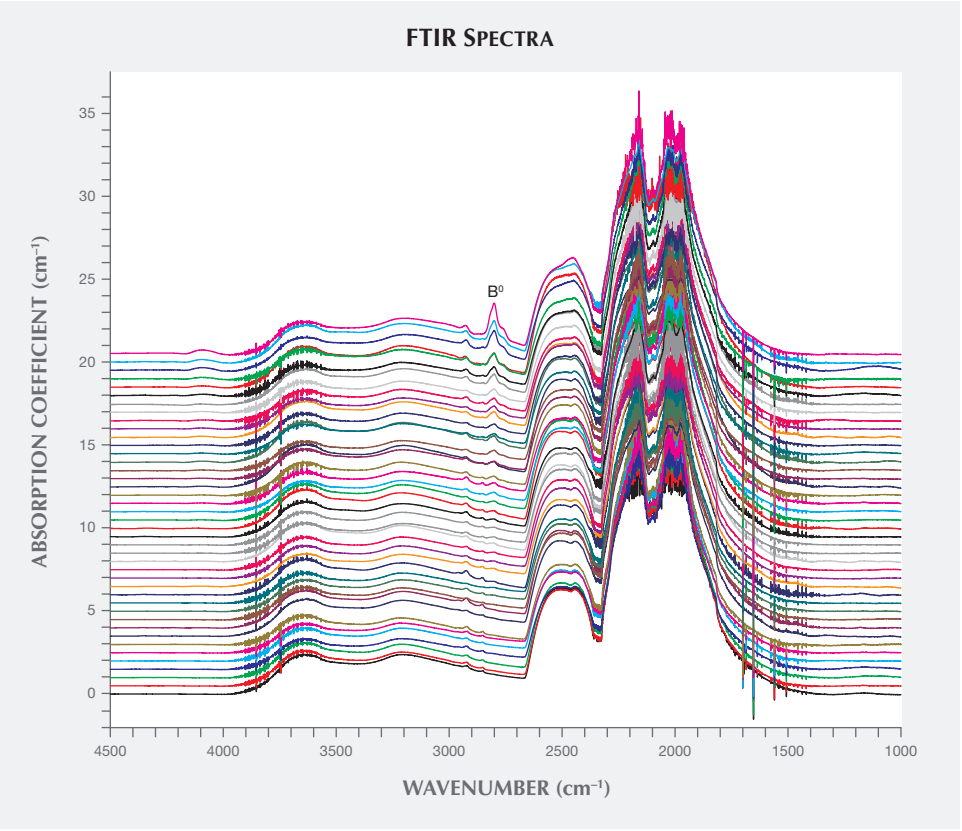

Figure 11. FTIR absorption spectroscopy revealed that 35 (80%) of the 44 synthetic diamonds contained detectable concentrations of neutral substitutional boron (B^0), with a characteristic absorption band centered at about 2800 cm^{-1}, and were thus classified as type IIb. Bulk B^0 concentrations for these synthetics are tabulated in table 1. The remaining samples did not show any boron- or nitrogen-related IR absorption and were classified as type IIa. The spectra are translated vertically for clarity. Traces for samples NDT-A and NDT-B are not shown due to poorer signal-to-noise ratio.

gen-related impurity content, with the resulting spectra shown in figure 11. For 35 (80%) of the HPHT synthetics, the only defect-related IR absorption seen was from neutral substitutional boron defects, which create an asymmetric absorption band at approximately 2800 cm^{-1}, resulting in a type IIb classification. Boron incorporation has been found to be growth sector–dependent in HPHT synthetic diamonds, with higher concentrations observed in {111} growth sectors (Burns et al., 1990). Consequently, the boron distribution across these multi-sector samples (as seen using DiamondView imaging) was also inhomogeneous. Their faceting made it impossible to conduct FTIR absorption experiments through single growth sectors. Nevertheless, to enable semi-quantitative comparison of the boron content between samples, bulk boron concentrations across complete volumes were calculated using the integrated intensities of the 2800 cm^{-1} band (Collins and Williams, 1971; Fisher et al., 2009). These results are tabulated in table 1, with bulk neutral boron concentrations up to 58 ± 9 ppb detected (NDT14, F color). The detection of boron is consistent with the phosphorescent behavior previously discussed. The remaining samples were assigned as type IIa because they did not show any defect-related absorption features. As these samples also exhibited identical phosphorescence, it is suggested that they contain boron centers at concentrations below the FTIR detection limit. It is important to note that these spectra are not unique to these samples, as colorless natural diamonds and HPHT- and CVD-grown synthetics can also be type IIa or type IIb.

Photoluminescence Spectroscopy. Photoluminescence spectra were collected for the samples immersed in liquid nitrogen (77 K) using excitation wavelengths of 324.8, 457.0, 488.0, 514.5, 632.5, and 830.0 nm, enabling the detection of defects that emit light from within the ultraviolet to infrared range. Data using the 324.8 and 488.0 nm lasers were not collected for samples NDT-A and NDT-B. Overall, the peaks reported here were generally weak, often detected only if the laser power was high enough to saturate the diamond Raman peak. Samples NDT21, NDT26, NDT33, NDT34, and NDT42, accounting for 11% of the suite, did not reveal any defect-related photoluminescence features.

The dominant photoluminescence features observed were nickel-related, with the 830.0 nm laser

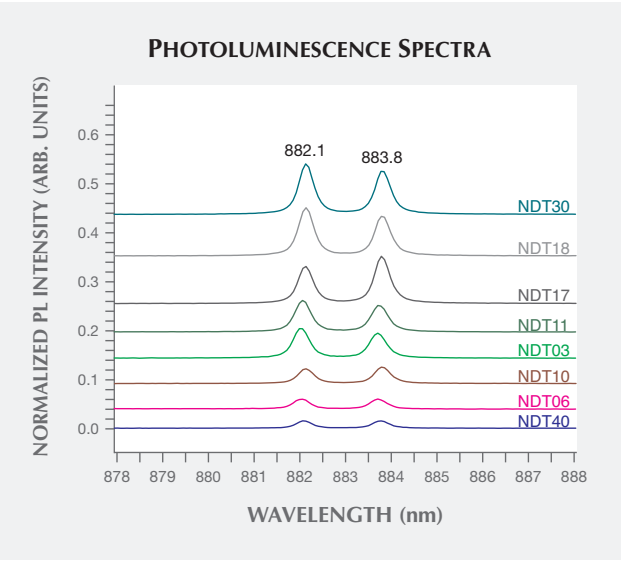

Figure 12. Representative photoluminescence spectra taken at liquid-nitrogen temperatures using 830.0 nm laser excitation revealed a Ni-related defect that produces a doublet with peaks at 882.1 and 883.8 nm in 32 (73%) of the New Diamond Technology samples. This doublet is thought to originate from the same Ni-related center that produces a doublet commonly reported at 1.4035/1.4008 eV (883.15/884.85 nm) for synthetic diamonds grown using Ni-containing solvent/catalyst melts. It is possible that the apparent energy shift resulted from an instrument calibration error. The 830.0 nm laser did not excite any other defect-related features. Once normalized to the unsaturated diamond Raman peak height, the spectra have been translated vertically for clarity.

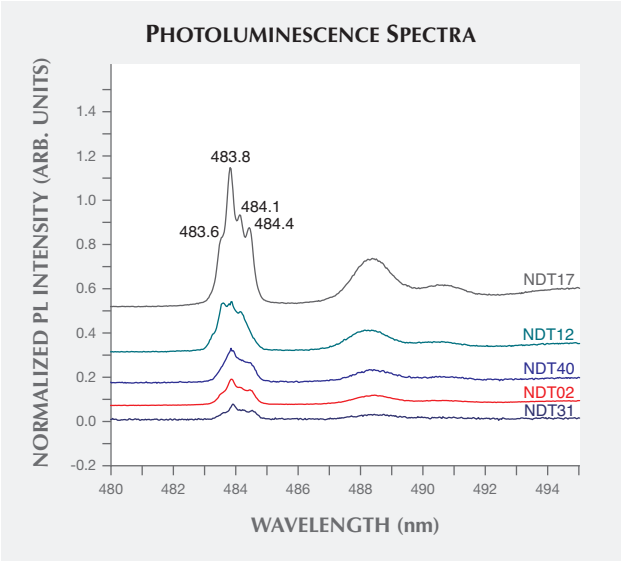

Figure 13. For 27 of the 42 samples, photoluminescence spectra collected at liquid-nitrogen temperatures using excitation from a 324.8 nm laser showed a multiplet with peaks at 483.6/483.8/484.1/484.4 nm. This feature is commonly thought to originate at a Ni-related center. For clarity, the Raman-normalized spectra for only five representative samples are shown, translated vertically to avoid overlap.

exciting a doublet at 882.1/883.8 nm (1.405/1.402 eV) in 32 samples (73%) and the 324.8 nm laser exciting a multiplet with lines at 483.6/483.8/484.1/484.4 nm (2.563/2.562/2.560/2.559 eV) in 27 samples. No comment can be made about whether samples NDT-A and NDT-B would show the latter multiplet, as no data was collected with the 324.8 nm excitation. Representative spectra, with the peak intensities normalized to the intensity of the unsaturated Raman peaks, are shown in figures 12 and 13. The 882.1/883.8 nm doublet is thought to be the one previously reported at 1.4035/1.4008 eV (883.15/884.85 nm), which is often referred to as the "1.40 eV center" (e.g., Nazaré et al., 1991; Yelisseyev and Kanda, 2007) where the shift in wavelength may be related to an instrument calibration error. The model for the 1.40 eV center is an interstitial Ni^+ atom distorted along a ⟨111⟩ direction (Nazaré et al., 1991). The separation of the peaks has been found to increase with increasing linewidths, suggesting that it is affected by strain levels. The 1.40 eV center is active in both photoluminescence and absorption, and is found exclusively in the {111} growth sectors in HPHT synthetic diamonds grown in the presence of Ni (Collins et al., 1990; Nazaré et al., 1991; Collins, 1992; Lawson and Kanda, 1993). Similarly, the 483.6/483.8/484.1/484.4 nm multiplet, also known as the "484 nm" or "2.56 eV" center, is commonly observed with photoluminescence in the {111} growth sectors of HPHT synthetic diamonds grown using Ni-based solvent/catalysts. Hence, it is also thought to be Ni-related, though its structure has yet to be determined (Dean, 1965; Collins et al., 1990; Collins, 1992; Nazaré et al., 1995). These nickel-related features indicate the presence of Ni in the solvent/catalyst melt used by NDT, intentional or otherwise.

Nitrogen-related features were only observed in the form of nitrogen-vacancy centers in the neutral (NV^0) and negative (NV^-) charge states with zero-phonon lines (ZPLs) at 575 (2.156 eV, not to be con-

fused with the phosphorescence band) and 637 nm (1.945 eV), respectively. These could be detected using either the 488.0 nm (not shown) or 514.5 nm lasers; figure 14 shows representative data using the latter excitation source. The features were weak, generally detectable only when the laser power was high enough to saturate the diamond Raman peak. The NV^0 ZPL, often more intense than that for NV^-, was detected in 26 (59%) of the samples. The NV^- ZPL was only seen in 11 (25%) samples. These features are common in both synthetic (type IIa and IIb) and natural (type IIa) diamonds. A feature at 503.2 nm (2.463 eV), possibly the H3 ($N\text{-}V\text{-}N^0$) defect, was not detected in any of the NDT synthetics using either 457.0 or 488.0 nm lasers. This feature was previously observed in near-colorless HPHT synthetics produced by AOTC (D'Haenens-Johansson et al., 2014).

The only remaining defect-related photoluminescence feature observed was the negative charge state of the silicon-vacancy center, SiV^-, which introduced a weak doublet ZPL at 736.6/736.9 nm (1.683/1.682 eV). SiV^-, which could be excited by the 488.0, 514.5, or 632.5 nm lasers (figure 15), was detected in 18 (41%) of the samples. Its presence is rare in HPHT synthetic diamonds, though it has been reported in intentionally doped samples studied by Clark et al. (1995) and Sittas et al. (1996), as well as in gem-quality HPHT synthetic samples of unknown origin (Moe and Wang, 2010; Wang and Moe, 2012) and those produced by AOTC (D'Haenens-Johansson et al., 2014). The low concentrations suggest that its presence may be unintentional.

It is noteworthy that some of the PL features that were weakly detected in several of the colorless and near-colorless HPHT synthetic diamonds grown by AOTC—with peaks at 658 (1.884 eV), 675.2 (1.836 eV), 706.9 (1.753 eV), 709.1 (1.748 eV), and 712.2 nm (1.740 eV)—were not observed in the samples produced by NDT (D'Haenens-Johansson et al., 2014). For the AOTC samples, these peaks were seen for diamonds grown in either BARS or toroid presses, which used different solvent/catalyst melts and nitrogen getters.

Figure 14. Twenty-six of the samples showed photoluminescence features attributed to nitrogen-vacancy centers, with the neutral (575 nm) charge state more intense than the negative (637 nm) charge state. These could be detected using either 488.0 or 514.5 nm laser excitation. These selected photoluminescence spectra, taken at liquid-nitrogen temperatures using 514.5 nm excitation, have been translated vertically for clarity. R *is the first-order Raman peak for diamond, the broad structure spanning 580–596 nm is the second-order Raman spectrum for diamond, and the sharp peak at 584.5 is the first-order Raman peak for liquid nitrogen, which is used to cool the samples.*

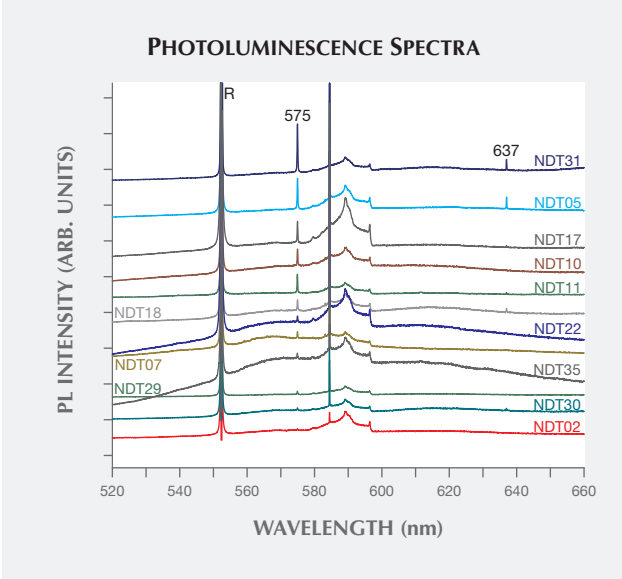

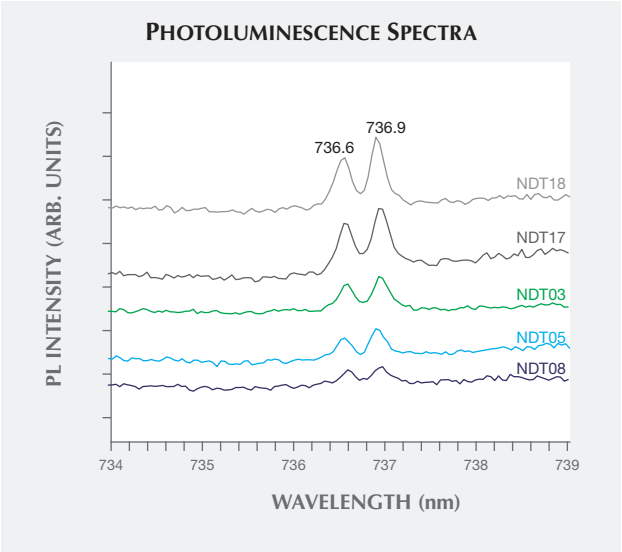

Figure 15. The negatively charged silicon-vacancy center, SiV^-, with emission at 736.6 and 736.9 nm, was weakly detected in 18 (41%) of the New Diamond Technology samples when using either 488.0, 514.5, or 633.0 nm laser excitation at liquid-nitrogen temperatures. The selected spectra presented here have been translated vertically for clarity.

DISCUSSION

Comparison with Other Gem-Quality Synthetics. Near-colorless and colorless synthetic diamonds of gem quality are produced using HPHT or CVD growth methods, with CVD material the most commonly encountered "white" synthetic diamond seen at GIA's laboratory. In recent years, advances in CVD growth methods and the introduction of post-growth decolorizing HPHT treatments have led to the rapid evolution of synthetic diamond quality. Production of colorless synthetics in modest sizes (approximately 0.30 ct) began around 2007 (Wang et al., 2007); by 2011, high-clarity samples weighing approximately 1 ct were widely available (Wang et al., 2012). While the size of CVD synthetics has continued to increase, the colors have been generally limited to near-colorless or faintly colored, and colorless grades are rare (Wang et al., 2013; Pure Grown Diamonds, 2015; Washington Diamonds Corp., 2013; D.NEA, 2015). The largest near-colorless CVD synthetic reported to date is a 3.16 ct sample with G color and SI_1 clarity, produced by Washington Diamonds Corp. (D.NEA, 2015), which was graded by a laboratory other than GIA. The record had previously been held by a 3.04 ct, I color, and SI_1 clarity CVD synthetic by Pure Grown Diamonds (formerly Gemesis), also graded by a non-GIA laboratory (Pure Grown Diamonds, 2014).

Conversely, HPHT growth for the gem trade was geared mainly toward fancy-color synthetic diamonds. Colorless gem-quality material has only been commercially available since 2012 (D'Haenens-Johansson et al., 2012, 2014). The main HPHT synthetic diamond producer in this sector is AOTC, whose colorless synthetics are polished to sizes up to 1 ct (AOTC, 2015). Although the D-Z diamond colors achieved by HPHT producers are typically closer to colorless than those by CVD producers, their material is generally smaller and may be visibly included. Outside of the gem industry, HPHT synthetic diamond producers such as Sumitomo Electric have reported growing 7–8 ct "rough" crystals described as "colorless" type IIa, though their material is intended for technological applications (Sumiya et al., 2002). If one further expands the search field to include unpolished colored HPHT synthetics, the largest reported in the literature is a 34.80 ct "yellow" specimen, grown solely for research purposes by De Beers (Koivula et al., 2000).

NDT's HPHT-grown synthetic gem diamonds in this investigation mark a dramatic improvement in the combination of colors and sizes attainable. Five colorless samples weighed over 2 ct, with clarities ranging from VVS_2 to I_2 (though this improved up to IF for smaller sizes). The 4.30 ct D-color, SI_1 clarity specimen (NDT-B) is the largest faceted laboratory-grown diamond of this color grade available to date (also reported by Poon et al., 2015), surpassing the largest CVD synthetic in both size and color known to the authors (while sharing the same clarity grade) (D.NEA, 2015). Although not studied for this investigation, a 10.02 ct E-color, VS_1 square-cut emerald HPHT-grown synthetic (graded by IGI), also by NDT, is so far the largest reported polished synthetic diamond grown using either HPHT or CVD technologies, of any color grade (International Gemological Institute, 2015; Wang and Moses, 2010; Poon et al., 2015; N.DEA, 2015). These results suggest that HPHT synthetic colorless gem-quality diamonds are now on a par with, and could potentially surpass, those produced by CVD methods.

Interestingly, AOTC uses both BARS and toroid presses, while NDT uses cubic presses (D'Haenens-Johansson et al., 2014). This demonstrates that different HPHT methodologies can yield comparable products, with NDT's cubic press methods currently yielding larger specimens. Like the AOTC synthetics, most of the NDT samples (80%) contained trace amounts of boron, peaking at a bulk concentration of 58 ± 9 ppb (NDT14). Meanwhile, the previously published bulk concentrations for representative AOTC samples were often higher, and in general the samples with higher boron concentrations had poorer color grades (further from colorless), introducing a blue hue that could produce grades up to Fancy Light blue, depending on the sample's size and faceting arrangement (D'Haenens-Johansson et al., 2014). DiamondView fluorescence images revealed that the intensity contrast between the different growth sectors was significantly weaker for the NDT specimens. These results may imply that the HPHT samples grown by NDT have a lower impurity content than those produced by AOTC, explaining the higher percentage of D–F color grades achieved (89% compared to 33%).

Identification Features. Although NDT sells its faceted synthetics with full disclosure of their origin, it is prudent to be aware of the relevant identification features in case these goods are at some point reintroduced into the gem trade without disclosure. NDT's gem-quality HPHT synthetics can be conclusively identified, though this often relies on a combination of gemological and spectroscopic observations. Sev-

eral of these characteristics are similar to those for HPHT synthetics from other sources.

Magnification may reveal the presence of metallic inclusions, which are not observed in CVD synthetic diamonds and are extremely rare, and with differing geometries, in natural diamonds (Sobolev et al., 1981). If sufficiently large or plentiful, the metallic inclusions can be confirmed by attraction to a strong magnet. Examination through crossed polarizers showed that the samples had extremely low strain levels, as indicated by low-order interference colors (blue and grays) and the inability to resolve a clear birefringence pattern. This is common for HPHT synthetics (Crowningshield, 1971) but in stark contrast to both CVD synthetic and natural stones, which show cross-hatched, mottled, or banded birefringence patterns, often in a variety of colors. The fluorescence and phosphorescence response of these HPHT synthetics was stronger to short-wave than long-wave UV, the opposite of the behavior seen in natural stones (Crowningshield, 1971; Shigley et al., 1997). Long-lasting phosphorescence, a characteristic rarely detected in natural diamonds, should be regarded with caution. If any of the above gemological observations are noted, further investigation using advanced testing techniques is crucial for conclusive origin determination.

The high-energy UV illumination from a DiamondView instrument will readily induce fluorescence in all diamonds, natural or synthetic. Inspection of the table, crown, and pavilion facets of the NDT samples revealed cuboctahedral growth sectors, which are characteristic of HPHT synthetics, though the pattern was very weak in some. Additionally, all the samples exhibited strong phosphorescence. A phosphorescence spectrometer could aid in their identification, as 13 of the 42 samples tested in this manner (31%) showed a phosphorescence band at approximately 575 nm, which has only been reported in certain HPHT-grown synthetic diamonds (Watanabe et al., 1997; Eaton-Magaña et al., 2008). Despite the similar emission wavelengths, this band should not be confused with the weak 580 nm band that has been infrequently detected for some natural type IIb diamonds. The 500 nm band, also observed, cannot be considered indicative of a synthetic origin, as it is often displayed by natural type IIb diamonds (Eaton-Magaña et al., 2007, 2008).

Further spectral analysis using FTIR absorption and PL spectroscopy may also be helpful. All the NDT samples were either type IIb or type IIa—i.e., they did not contain detectable amounts of isolated or aggregated nitrogen defects. Natural, treated, and CVD or HPHT synthetic colorless diamonds can all belong to these types. Since some 98% of natural diamonds contain A-aggregates (nitrogen pairs, which absorb at approximately 1280 cm^{-1}), their absence from a sample's IR spectrum would indicate a need for detailed analysis. PL, like FTIR, cannot alone conclusively identify an HPHT synthetic, yet it was effective at revealing suspicious impurities. The Ni-related features observed at 882.1/883.8 nm (1.405/1.402 eV) and at 483.6/483.8/484.1/484.4 nm (2.563/2.562/2.560/2.559 eV) are seldom detected for natural type IIa and IIb diamonds and have not been reported for CVD synthetics (Nobel et al., 1998; Chalain, 2003). The 736.6/736.9 nm (1.683/1.682 eV) SiV^- feature, often used in the identification of CVD-grown samples, has been detected only rarely in natural diamonds or in other HPHT synthetics (Breeding and Wang, 2008; Moe and Wang, 2010; Wang and Moe, 2012; D'Haenens-Johansson et al., 2014). A weak SiV^- feature was detected in a subset of the specimens in this study. Its presence remains a source of concern, though a stone with this feature could be either natural or CVD synthetic.

CONCLUSIONS

New Diamond Technology's colorless HPHT-grown synthetic diamonds are being faceted into gems for the jewelry trade. This study of 44 representative samples revealed that the company can create faceted colorless and faintly colored synthetics weighing up to 4.30 ct and 5.11 ct, respectively. Although the samples spanned the full range of clarity, NDT has demonstrated the capacity to produce high clarities. One such specimen, a 1.13 ct round brilliant with a very good cut grade, characterized by D color and IF clarity, was remarkable for its quality. All indications point to high-color and high-clarity HPHT synthetics becoming more prominent in the gem trade. The colorless stones in the study are comparable to top-quality natural diamonds and surpass (for this color range) the sizes achieved by alternative producers. NDT's continued focus on expanding production and increasing the sizes of their colorless samples emphasizes the need for awareness by grading laboratories, members of the diamond trade, and consumers. Through careful analysis using gemological, fluorescence, and spectroscopic methods, these products can be confidently identified as synthetic, thus posing no threat to a well-informed, responsible, and transparent diamond trade.

ABOUT THE AUTHORS
Dr. D'Haenens-Johansson (ujohansson@gia.edu) is a research scientist, Mr. Moe is a research associate, Mr. Johnson is the supervisor of diamond advanced testing, and Dr. Wang is the director of research and development at GIA's New York laboratory. Dr. Katrusha is a scientific partner of New Diamond Technology, Ltd.

ACKNOWLEDGMENTS
The authors are grateful to Tamazi Khikhinashvili and Aleko Arens from New Diamond Technology, in St. Petersburg, Russia, for providing HPHT-grown synthetic diamonds for this investigation. Brian Bujarski, formerly a technician at GIA's New York laboratory, is thanked for his help with PL data acquisition.

REFERENCES

AOTC (2015) Synthetic white diamonds, http://aotc.com/unique/white-diamonds [date accessed: Feb. 23, 2015].

Bates R. (2015) Company claims to have produced 5 carat synthetic diamond, *JCK Magazine*, Feb. 17, http://www.jckonline.com/2015/02/17/company-claims-to-have-produced-5-carat-synthetic-diamond.

Bovenkerk H.P., Bundy F.P., Hall H.T., Strong H.M., Wentorf R.H. (1959) Preparation of diamond. *Nature*, Vol. 194, No. 4693, pp. 1094–1098, http://dx.doi.org/10.1038/1841094a0.

Breeding C.M., Wang W. (2008) Occurrence of the Si-V defect center in natural colorless gem diamonds. *Diamond and Related Materials,* Vol. 17, Nos. 7–10, pp. 1335–1344, http://dx.doi.org/10.1016/j.diamond.2008.01.075.

Burns R.C., Cvetkovic V., Dodge C. N., Evans D.J.F., Rooney M.-L.T., Spear P.M., Welbourn C.M. (1990) Growth-sector dependence of optical features in large synthetic diamonds. *Journal of Crystal Growth*, Vol. 104, No. 2, pp. 257–279, http://dx.doi.org/10.1016/0022-0248(90)90126-6.

Chalain J.P. (2003) Gem News International: A natural yellow diamond with nickel-related optical centers. *G&G*, Vol. 39, No. 4, pp. 325–326.

Clark C.D., Kanda H., Kiflawi I., Sittas G. (1995) Silicon defects in diamond. *Physical Review B*, Vol. 51, No. 23, pp. 16681–16688, http://dx.doi.org/10.1103/PhysRevB.51.16681.

Collins A.T., Williams A.W.S. (1971) The nature of the acceptor centre in semiconducting diamond. *Journal of Physics C: Solid State Physics*, Vol. 4, pp. 1789–1800, http://dx.doi.org/10.1088/0022-3719/4/13/030.

Collins A.T., Kanda H., Burns R.C. (1990) The segregation of nickel-related optical centers in the octahedral growth sectors of synthetic diamond. *Philosophical Magazine Part B*, Vol. 61, No. 5, pp. 797–810, http://dx.doi.org/10.1080/13642819008207562.

Collins A.T. (1992) The characterisation of point defects in diamond by luminescence spectroscopy. *Diamond and Related Materials*, Vol. 1, Nos. 5–6, pp. 457–469, http://dx.doi.org/10.1016/0925-9635(92)90146-F.

Crowningshield R. (1971) General Electric's cuttable synthetic diamonds. *G&G*, Vol. 13, No. 10, pp. 302–314.

Dean P.J. (1965) Bound excitons and donor-acceptor pairs in natural and synthetic diamond. *Physical Review*, Vol. 139, No. 2A, pp. A588–A602, http://dx.doi.org/10.1103/PhysRev.139.A588.

Dean P.J. (1973) Inter-impurity recombinations in semiconductors. *Progress in Solid State Chemistry*, Vol. 8, pp. 1–126, http://dx.doi.org/10.1016/0079-6786(73)90004-6.

D'Haenens-Johansson U.F.S., Moe K.S., Johnson P., Wong S.Y., Wang W. (2012) Lab Notes: Near-colorless HPHT-grown synthetic diamonds from Advanced Optical Technology Co. *G&G*, Vol. 48, No. 2, p. 141.

D'Haenens-Johansson U.F.S., Moe K.S., Johnson P., Wong S.Y., Lu R., Wang W. (2014) Near-colorless HPHT synthetic diamonds from AOTC Group. *G&G*, Vol. 50, No. 1, pp. 30–45, http://dx.doi.org/10.5741/GEMS.50.1.30.

D.NEA (2015) 3.16 ct G color round cut created diamond, http://d.neadiamonds.com/lab-created-diamonds/WB1225.

Eaton-Magaña S., Post J.E., Heaney P.J., Walters R.A., Breeding C.M., Butler J.E. (2007) Fluorescence spectra of colored diamonds using a rapid, mobile spectrometer. *G&G*, Vol. 43, No. 4, pp. 332–351, http://dx.doi.org/10.5741/GEMS.43.4.332.

Eaton-Magaña S., Post J., Heaney P.J., Freitas J., Klein P., Walters R., Butler J.E. (2008) Using phosphorescence as a fingerprint for the Hope and other blue diamonds. *Geology*, Vol. 36, No. 1, pp. 83–86, http://dx.doi.org/10.1130/G24170A.1.

Eaton-Magaña S., Lu R. (2011) Phosphorescence in type IIb diamonds. *Diamond and Related Materials*, Vol. 20, No. 7, pp. 983–989, http://dx.doi.org/10.1016/j.diamond.2011.05.007.

Fisher D., Sibley S.J., Kelly C.J. (2009) Brown colour in natural diamond and interaction between the brown related and other colour-inducing defects. *Journal of Physics: Condensed Matter*, Vol. 21, No. 36, 364213, 10 pp., http://dx.doi.org/10.1088/0953-8984/21/36/364213.

Hall M., Lu R., Wang W. (2010) U.S. Patent No. US 2010/0220311A1. Issued September 2.

International Gemological Institute (2015) International Gemological Institute (IGI) Hong Kong certifies record-breaking, world's largest colorless grown diamond, May 26, http://igi-worldwide.com/igi-certifies-worlds-largest-colorless-grown-diamond.html.

Klein P.B., Crossfield M.D., Freitas J.A., Collins A.T. (1995) Donor-acceptor pair recombination in synthetic type-IIb semiconducting diamond. *Physical Review B*, Vol. 51, No. 15, pp. 9634–9642, http://dx.doi.org/10.1103/PhysRevB.51.9634.

Koivula J.I., Tannous M. Schmetzer K. (2000) Synthetic gem materials and simulants in the 1990s. *G&G*, Vol. 36, No. 4, pp. 360–379, http://dx.doi.org/10.5741/GEMS.36.4.360.

Lawson S.C., Kanda H. (1993) An annealing study of nickel point defects in high-pressure synthetic diamond. *Journal of Applied Physics*, Vol. 73, No. 8, pp. 3967–3973, http://dx.doi.org/10.1063/1.352861.

Martineau P.M., Lawson S.C., Taylor A.J., Quinn S.J., Evans D.J.F., Crowder M.J. (2004) Identification of synthetic diamond grown using chemical vapor deposition (CVD). *G&G*, Vol. 40, No. 1, pp. 2–25, http://dx.doi.org/10.5741/GEMS.40.1.2.

Moe K.S., Wang W. (2010) Lab Notes: Silicon-vacancy defect found in blue HPHT-grown synthetic diamond. *G&G*, Vol. 46, No. 4, p. 302.

Nazaré M.H., Neves A.J., Davies G. (1991) Optical studies of the 1.40-

eV Ni center in diamond. *Physical Review B*, Vol. 43, No. 17, pp. 14196–14205, http://dx.doi.org/10.1103/PhysRevB.43.14196.
Nazaré M.H., Mason P.W., Watkins G.D., Kanda H. (1995) Optical detection of magnetic resonance of nitrogen and nickel in high-pressure synthetic diamond. *Physical Review B*, Vol. 51, No. 23, pp. 16741–16745, http://dx.doi.org/10.1103/PhysRevB.51.16741.
Nobel C.J., Pawlik T., Spaeth J.-M. (1998) Electron paramagnetic resonance investigations of nickel defects in natural diamonds. *Journal of Condensed Matter*, Vol. 10, No. 50, pp. 11781–11794, http://dx.doi.org/10.1088/0953-8984/10/50/017.
Palik E.D. (1985) *Handbook of Optical Constants of Solids*. Academic Press, London.
Poon P.Y., Wong S.Y., Lo C. (2015) Large HPHT-grown synthetic diamonds examined in GIA's Hong Kong laboratory. *GIA Research & News*, Mar. 16, http://www.gia.edu/gia-news-research-large-hpht-grown-synthetic-diamonds-examined-in-gia-hong-kong-laboratory.
Pure Grown Diamonds (2014) World's largest laboratory pure grown diamond unveiled. *Business Wire*, Dec. 30, http://www.businesswire.com/news/home/20141229005491/en/adding-multimedia-worlds-largest-laboratory-pure-grown#.votnbs63raq.
Pure Grown Diamonds (n.d.) Lab grown diamonds, http://www.puregrowndiamonds.com/diamonds/single [date accessed: Jun. 23, 2015].
Rooney M.-L.T., Welbourn C.M., Shigley J.E., Fritsch E., Reinitz I. (1993) De Beers near colorless-to-blue experimental gem-quality synthetic diamonds. *G&G*, Vol. 29, No. 1, pp. 38–45, http://dx.doi.org/10.5741/GEMS.29.1.38.
Satoh S., Sumiya H., Tsuji K., Gouda Y. (2000) US Patent No. US006129900A. Issued October 10.
Shigley J.E., Moses T.M., Reinitz I., Elen S., McClure S.F., Fritsch E. (1997) Gemological properties of near-colorless synthetic diamonds. *G&G*, Vol. 33, No. 1, pp. 42–53, http://dx.doi.org/10.5741/GEMS.33.1.42.
Shigley J.E., McClure S.F., Breeding C.M. Shen A.H.-T., Muhlmeister M. (2004) Lab-grown colored diamonds from Chatham Created Gems. *G&G*, Vol. 40, No. 2, pp. 128–145, http://dx.doi.org/10.5741/GEMS.40.2.128.
Sittas G., Kanda H., Kiflawi I., Spear P.M. (1996) Growth and characterization of Si-doped diamond single crystals grown by the HTHP method. *Diamond and Related Materials*, Vol. 5, Nos. 6–8, pp. 866–869, http://dx.doi.org/10.1016/0925-9635(95)00449-1.
Sobolev N.V., Efimiva E.S., Pospelova L.N. (1981) Native iron in diamonds of Yakutia and its paragenesis. *Soviet Geology and Geophysics*, Vol. 22, No. 12, pp. 18–21.
Strong H.M. (1977) US Patent No. US40142673. Issued August 16.
Strong H.M., Chrenko R.M. (1971) Further studies on diamond growth rates and physical properties of laboratory-made diamond. *The Journal of Physical Chemistry*, Vol. 75, No. 12, pp. 1838–1843, http://dx.doi.org/10.1021/j100681a014.
Sumiya H. (2009) Recent advances in high pressure apparatus for diamond synthesis. *The Review of High Pressure Science and Technology*, Vol. 19, No. 4, pp. 264–269, http://dx.doi.org/10.4131/jshpreview.19.264 [in Japanese].
Sumiya H., Satoh S. (1996) High-pressure synthesis of high-purity diamond crystal. *Diamond and Related Materials*, Vol. 5, pp. 1359–1365, http://dx.doi.org/10.1016/0925-9635(96)00559-6.
Sumiya H., Toda N., Satoh S. (2002) Growth rate of high-quality large diamond crystals. *Journal of Crystal Growth*, Vol. 237–239, Part 2, pp. 1281–1285, http://dx.doi.org/10.1016/S0022-0248(01)02145-5.
Sumiya H., Toda N., Satoh S. (2005) Development of high-quality large-size synthetic diamond crystals. *SEI Technical Review*, Vol. 60, pp. 10–16.
Wang W., Moses T. (2010) Lab Notes: Large (4+ ct) yellow-orange HPHT-grown synthetic diamond. *G&G*, Vol. 46, No. 4, p. 301.
Wang W., Moe K.S. (2012) Lab Notes: Silicon-vacancy defect in HPHT-grown type IIb synthetic. *G&G*, Vol. 48, No. 4, pp. 304–305.
Wang W., Hall M.S., Moe K.S., Tower J., Moses T.M. (2007) Latest-generation CVD-grown synthetic diamonds from Apollo Diamond Inc. *G&G*, Vol. 43, No. 4, pp. 294–312, http://dx.doi.org/10.5741/GEMS.43.4.294.
Wang W., D'Haenens-Johansson U.F.S., Johnson P., Moe K.S., Emerson E., Newton M.E., Moses T.M. (2012) CVD synthetic diamonds from Gemesis Corp. *G&G*, Vol. 48, No.2, pp. 80–97, http://dx.doi.org/10.5741/GEMS.43.4.294.
Wang W., Moe K.S., Yeung S.F., D'Haenens-Johansson, U. (2013) Lab Notes: Very large CVD-grown. *G&G*, Vol. 49, No. 1, p 50.
Watanabe K., Lawson S.C., Isoya J., Kanda H., Sato Y. (1997) Phosphorescence in high-pressure synthetic diamond. *Diamond and Related Materials*, Vol. 6, No. 1, pp. 99–106 http://dx.doi.org/10.1016/S0925-9635(96)00764-9.
Washington Diamonds Corp. (2013) Going where no diamond-produing lab has gone before: A true colorless, one carat, lab grown CVD diamond, Oct. 3, http://www.washingtondiamondscorp.com/going-where-no-diamond-producing-lab-has-gone-before-a-true-colorless-one-carat-lab-grown-cvd-diamond/
Welbourn C.M., Cooper M., Spear P.M. (1996) De Beers natural versus synthetic diamond verification instruments, *G&G*, Vol. 32, No. 3, pp. 156–169, http://dx.doi.org/10.5741/GEMS.32.3.156.
Yelisseyev A., Kanda H. (2007) Optical centers related to 3d transition metals in diamond. *New Diamond and Frontier Carbon Technology*, Vol. 17, No. 3, pp. 127–178.
Zhan-Chang L., Xiao-Peng J., Guo-Feng H., Mei-Hua H. Yong L., Bing-Min Y. (2013) FEM simulations and experimental studies of the temperature field in a large diamond crystal growth cell. *Chinese Physics B*, Vol. 22, No. 1, 014701–014706, http://dx.doi.org/10.1088/1674-1056/22/1/014701.
Zhu H., Pearson K., Kim J.R. (2012) US Patent No. US2012/0192785A1. Issued August 2.